Int. J. Heat Mass Transfer. Vol. 34, No. 1, pp. 69–78, 1991
Printed in Great Britain

0017–9310/91 $3.00+0.00

Analysis of heat transfer in a pipe carrying two-phase gas–particle suspension

KEE SOO HAN, HYUNG JIN SUNG and MYUNG KYOON CHUNG
Department of Mechanical Engineering, Korea Advanced Institute of Science and Technology, P.O. Box 150, Cheongryang, Seoul, Korea

(*Received* 11 *October* 1989 *and in final form* 26 *March* 1990)

Abstract—A 'two-fluid model' using the thermal eddy diffusivity concept and Lumley's drag reduction theory, is proposed to analyse heat transfer of the turbulent dilute gas–particle flow in a vertical pipe with constant wall heat flux. The thermal eddy diffusivity model is derived to be a function of the ratio of the heat capacity–density products $\bar{\rho}C_p$ of the gaseous phase and the particulate phase and also of the ratio of the thermal relaxation time scale to that of turbulence. Lumley's theory is applied to find the variation of the viscous sublayer thickness depending on the particle loading ratio Z and the relative particle size d_p/D. At low loading ratio, the size of the viscous sublayer thickness is important for suspension heat transfer, while at higher loading, the effect of the ratio $\overline{\rho_p}C_{p_p}/\overline{\rho_f}C_{p_f}$ is dominant. The major cause of decrease in the suspension Nusselt number at low loading ratio is found to be due to the increase of the viscous sublayer thickness caused by the suppression of turbulence near the wall by the presence of solid particles. Predicted Nusselt numbers using the present model are in satisfactory agreement with available experimental data both in the pipe entrance and the fully developed regions.

INTRODUCTION

IT IS WELL known that the addition of small solid particles to a gas flow in a pipe either increases or decreases the heat transfer through the pipe wall. However, there is still great controversy in explaining the effect of the presence of small particles on the heat transfer. Farbar and Morley [1] and Wilkinson and Norman [2] reported that the suspension Nusselt numbers were significantly increased by the addition of solid particles. On the contrary, Farbar and Depew [3], Depew and Farbar [4], Wahi [5], and Boothroyd and Haque [6, 7] found that it first decreases to a minimum value at a certain low solids–gas loading ratio and then increases with the loading ratio. Such a complicated variation of the heat transfer coefficient in the gas–particle suspension flow is not yet systematically understood. Only empirical correlations are hitherto available for estimation of the suspension Nusselt number through the pipe wall.

Recently, Kane and Pfeffer [8] explained the reduction phenomenon of the suspension Nusselt number by a thickening mechanism of the viscous sublayer under particle presence. On the other hand, Tien [9] who first analytically treated suspension heat transfer, found that the presence of the particles in the flowing stream prolongs the thermal entrance region and that the rate of heat transfer is governed by the heat capacity–density ratio $\overline{\rho_p}C_{p_p}/\overline{\rho_f}C_{p_f}$; increase of the ratio augments the suspension heat transfer.

Michaelides and Lasek [10, 11] developed one-dimensional models to describe the behaviour of particles in air flow. However, because they used an experimental correlation about the augmentation of the suspension heat transfer, the reduction of the suspension heat transfer could not be predicted by their model. Abou-Arab and Abou-Ellail [12, 13] applied a recently developed two-phase k–ε model to analyse the heat and momentum transfers. The two-phase k–ε model yielded only slight reduction in heat transfer. Recently, the present authors [14] modified Lee and Chung's model [15] with Lumley's drag reduction viscous sublayer theory [16] to analyse the momentum transfer of Boothroyd's experiments [17]. Their results showed the correct reduction behaviour of the drag in gas–particle flows.

The objective of this study is to extend the analysis of the previous study of the present authors [14] to investigate the heat transfer characteristics of an upward gas–particles flow for various relative particle sizes d_p/D and loading ratios in a vertical pipe under a uniform heat flux condition.

GOVERNING EQUATIONS FOR GAS–PARTICLE SUSPENSION FLOW

In the present study, the 'two-fluid model' approach is adopted to analyse the heat transfer in a vertical pipe which carries small size particles at relatively low particle loading. The concept and the limitation on the two-fluid model is described in detail in Ishii [18].

The volume-averaged continuity, momentum, and energy equations for both phases in cylindrical coordinates can be obtained in the following forms by performing the conventional Reynolds averaging of their governing equations for an instantaneous field [18, 19].

The mean governing equations for the gaseous phase (f) are:

NOMENCLATURE

A	cross-sectional area of pipe
A^+	van Driest damping constant
A^+_{DR}	drag reduction viscous sublayer thickness
C_p	specific heat for constant pressure
D	pipe diameter or van Driest damping function
d_p	particle diameter
F_{px}, F_{pr}	Stokesian drag forces in the axial and radial directions
g	gravitational acceleration
h_s	local heat transfer coefficient for suspension flow
K_θ	model constant
$\hat{K}_d$	ratio of viscous cutoff wave number under particle loading to that in the clean fluid
k_f	thermal conductivity for the gaseous phase
l_f	characteristic length scale for the gaseous phase flow
Nu	Nusselt number
Nu_s	suspension Nusselt number
P	static pressure
Pr_T	turbulent Prandtl number
Q_p	heat transferred from the particulate phase to the gaseous phase
$\hat{q}''$	local pipe wall heat flux
Re	Reynolds number based on pipe diameter
Re_p	particle Reynolds number
r	radial distance from the pipe axis
s	viscous cutoff frequency
$\hat{s}$	ratio of viscous cutoff frequency under particle loading to that in the clean fluid
T	averaged mean temperature
t_l	Lagrangian integral time scale
t^*	particle relaxation time scale
U, V	average mean velocity components in the axial and radial directions
u', v'	fluctuating velocity components in the axial and radial directions
W	mass flux
x	axial distance
y	distance from the wall
Z	solids–gas loading ratio, W_p/W_f.

Greek symbols

α	volume fraction
α_{fl}	laminar thermal diffusivity of the gaseous phase
δ_{99}	boundary layer thickness
$\hat{\delta}$	ratio of sublayer thickness under particle loading to that in the clean fluid
ε	dissipation rate
ε_f, ε_p	kinematic eddy viscosities
θ	fluctuating temperature
κ	von Karman constant
λ_f, λ_p	thermal eddy diffusivities
ν_{fl}, ν_{pl}	kinematic laminar viscosities of the gaseous and particulate phases
ρ_f	density of gas
ρ_s	density of particle
ρ_f	bulk density of gaseous phase, $\rho_f(1-\alpha)$
ρ_p	bulk density of particulate phase, $\rho_s\alpha$
τ^*	thermal characteristic time scale.

Subscripts

c	pipe centre
DR	drag reduction
f	gaseous phase
l	laminar
o	clean fluid
p	particle laden, or particulate phase, or bulk property
s	solid
w	wall.

Superscripts

+	non-dimensionalized wall coordinate
^	ratio of relevant physical quantities of suspension fluid to clean fluid
′	fluctuating quantity.

$$\frac{\partial}{\partial x}[\rho_f(1-\alpha)U_f]+\frac{1}{r}\frac{\partial}{\partial r}[r\rho_f(1-\alpha)V_f]=\frac{1}{r}\frac{\partial}{\partial r}[r\rho_f\overline{\alpha' v_f'}] \tag{1}$$

$$\rho_f(1-\alpha)\left[U_f\frac{\partial U_f}{\partial x}+V_f\frac{\partial U_f}{\partial r}\right]$$
$$=-(1-\alpha)\frac{\partial P}{\partial x}-\rho_f(1-\alpha)g$$
$$+\frac{1}{r}\frac{\partial}{\partial r}\left[r\rho_f(1-\alpha)\left(\nu_{fl}\frac{\partial U_f}{\partial r}-\overline{u_f'v_f'}\right)\right]$$
$$+F_{px}+\rho_f\overline{\alpha' v_f'}\frac{\partial U_f}{\partial r}+\frac{\partial}{r\partial r}[r\rho_f\overline{\alpha' u_f'}V_f] \tag{2}$$

$$\rho_f(1-\alpha)\left[U_f\frac{\partial V_f}{\partial x}+V_f\frac{\partial V_f}{\partial r}\right]=-(1-\alpha)\frac{\partial P}{\partial r}$$
$$+\frac{1}{r}\frac{\partial}{\partial r}\left[r\rho_f(1-\alpha)\left(\nu_{fl}\frac{\partial V_f}{\partial r}-\overline{v_f'^2}\right)\right]$$
$$-\frac{1}{r}\rho_f(1-\alpha)\left(\nu_{fl}\frac{V_f}{r}-\overline{w_f'^2}\right)+F_{pr}+\rho_f\overline{\alpha' v_f'}\frac{\partial V_f}{\partial r}$$
$$+\frac{\partial}{\partial x}[\rho_f\overline{\alpha' v_f'}U_f]+\frac{\partial}{r\partial r}[r\rho_f\overline{\alpha' v_f'}V_f] \tag{3}$$

$$\rho_f(1-\alpha)C_{p_f}\left[U_f\frac{\partial T_f}{\partial x}+V_f\frac{\partial T_f}{\partial r}\right]$$
$$=\frac{1}{r}\frac{\partial}{\partial r}\left[r(1-\alpha)\left(k_f\frac{\partial T_f}{\partial r}-\rho_f C_{p_f}\overline{\theta_f' v_f'}\right)\right]$$
$$+(U_p-U_f)F_{px}+(V_p-V_f)F_{pr}+Q_p+\rho_f C_{p_f}\overline{\alpha' v_f'}\frac{\partial T_f}{\partial r}. \quad (4)$$

The mean governing equations for the secondary particulate phase (p) are:

$$\frac{\partial}{\partial x}[\rho_s\alpha U_p]+\frac{1}{r}\frac{\partial}{\partial r}[r\rho_s V_p]=-\frac{1}{r}\frac{\partial}{\partial r}[r\rho_s\overline{\alpha' v_p'}] \quad (5)$$

$$\rho_s\alpha\left[U_p\frac{\partial U_p}{\partial x}+V_p\frac{\partial U_p}{\partial r}\right]=-\alpha\frac{\partial P}{\partial x}-(\rho_s-\rho_f)\alpha g$$
$$+\frac{1}{r}\frac{\partial}{\partial r}\left[r\rho_s\alpha\left(v_{pl}\frac{\partial U_p}{\partial r}-\overline{u_p' v_p'}\right)\right]-F_{px}$$
$$-\rho_s\overline{\alpha' v_p'}\frac{\partial U_p}{\partial r}-\frac{\partial}{r\partial r}[r\rho_s\overline{\alpha' u_p'}V_p] \quad (6)$$

$$\rho_s\alpha\left[U_p\frac{\partial V_p}{\partial x}+V_p\frac{\partial V_p}{\partial r}\right]=-\alpha\frac{\partial P}{\partial r}$$
$$+\frac{1}{r}\frac{\partial}{\partial r}\left[r\rho_s\alpha\left(v_{pl}\frac{\partial V_p}{\partial r}-\overline{v_p'^2}\right)\right]$$
$$-\frac{1}{r}\rho_s\alpha\left(v_{pl}\frac{V_p}{r}-\overline{w_p'^2}\right)-F_{pr}-\rho_s\overline{\alpha' v_p'}\frac{\partial V_p}{\partial r}$$
$$-\frac{\partial}{\partial x}[\rho_s\overline{\alpha' v_p'}U_p]-\frac{\partial}{r\partial r}[r\rho_s\overline{\alpha' v_p'}V_p] \quad (7)$$

$$\rho_s\alpha C_{p_p}\left[U_p\frac{\partial T_p}{\partial x}+V_p\frac{\partial T_p}{\partial r}\right]$$
$$=\frac{1}{r}\frac{\partial}{\partial r}[-\rho_s r\alpha C_{p_p}\overline{\theta_p' v_p'}]-Q_p-\rho_s C_{p_p}\overline{\alpha' v_p'}\frac{\partial T_p}{\partial r}. \quad (8)$$

Heat transfer by radiation is neglected for the present study in which the temperature difference between the gaseous and particulate phases is assumed small.

In the momentum equations for both phases, F_{px} and F_{pr} are the interaction forces between both phases in the axial and radial directions which are approximated by the Stokes drag law with a correction factor due to the presence of the wall [14, 20]. In the energy equations Q_p is the heat transferred from the particulate phase to the gaseous phase. Similar to the interaction forces, the interactive heat transfer Q_p is proportional to the temperature difference [21]

$$Q_p=\frac{\rho_s}{\tau^*}\alpha C_{p_p}(T_p-T_f) \quad (9)$$

where τ^* is the thermal relaxation time which is defined and approximated by

$$\tau^*\equiv\frac{d_p^2\rho_s C_{p_p}}{6Nu_p k_f}=3\left(\frac{Pr_f}{Nu_p}\right)\left(\frac{C_{p_p}}{C_{p_f}}\right)t^*[1+0.15Re_p^{0.687}]. \quad (10)$$

Here, C_{p_f} and C_{p_p} are the specific heats of the gaseous and particulate phases, respectively, for constant pressure and t^* is the particle relaxation time. Further, the particle Nusselt number for the small particle Reynolds number is represented by the correlation formula [22]

$$Nu_p=2+0.6Re_p^{0.5}\,Pr_f^{0.33} \quad (11)$$

which is known to be valid for $Re_p<700$.

TURBULENCE MODELS FOR GAS–PARTICLE SUSPENSION FLOW

The turbulence closures for the time averaged products $\overline{u_f' v_f'}$, $\overline{u_p' v_p'}$, $\overline{\alpha' v_f'}$, and $\overline{\alpha' v_p'}$ are made by assuming scalar eddy diffusivities, ε_f and ε_p, for the gaseous and particulate phases, respectively, the derivations of which are explained in detail in a previous paper [15]. At the same level of closure, the turbulent heat transfer correlations may be represented by the following scalar transport hypothesis:

$$\overline{v_f'\theta_f'}=-\lambda_f\frac{\partial T_f}{\partial r} \quad (12)$$

$$\overline{v_p'\theta_p'}=-\lambda_p\frac{\partial T_p}{\partial r} \quad (13)$$

where λ_f and λ_p are the thermal eddy diffusivities of the gaseous and the particulate phases, respectively.

Eddy viscosity models

The ratio of the scalar eddy viscosity in the particle laden flow ε_f to that in the clean gas flow ε_{fo} is approximated by a model derived in ref. [15] which is based on the assumption of the state of local equilibrium between the production and dissipation of the turbulent kinetic energy for the gaseous phase

$$\frac{\varepsilon_f}{\varepsilon_{fo}}=\left[\frac{1}{1+C'_{p\varepsilon}\dfrac{\overline{\rho_p}}{\rho_f}\dfrac{t_l}{t^*}\left(1-\dfrac{\varepsilon_p}{\varepsilon_f}\right)}\right]^{1/2} \quad (14)$$

where t_l is the turbulent time scale and $C'_{p\varepsilon}$ is a model constant of about 3.5.

The eddy viscosity of clean gas flow ε_{fo} is estimated from the mixing length model using the van Driest damping function D as

$$\varepsilon_{fo}=\kappa^2(R-r)^2D^2\frac{dU_f}{dr} \quad \text{for } (R-r)<\frac{\zeta\delta_{.99}}{\kappa} \quad (15)$$

$$=a\,Re^b\,\nu_{fl} \quad \text{for } (R-r)>\frac{\zeta\delta_{.99}}{\kappa} \quad (16)$$

where ζ is selected such that the numerical value of ε_{fo}

should be matched smoothly between equations (15) and (16) at their interface.

The van Driest damping function D in equation (15) is given by

$$D = (1-\exp(-y^+/A^+)). \quad (17)$$

In the previous study [14] using Lumley's drag reduction model [16] for the analysis of momentum transfer in two-phase pipe flows, it has been shown that the damping 'constant' A^+ which represents the effective non-dimensional thickness of the viscous sublayer depends on the loading ratio, the particle relaxation time scale and the Kolmogoroff time scale. The same approach for estimating A^+ in ref. [14] is used in the present study, which is rather briefly summarized as follows.

When the frequency of the particle inertia phenomena ($\approx 1/t^*$) is smaller than the viscous cutoff frequency s, the rate of energy dissipation for gas–particle suspension flow is modelled as follows [14]:

$$\frac{\nu_{fl}}{1+Z}s^2 + 1.8C_\varepsilon'\varepsilon(\pi/2 - 1/0.74st^*)\frac{Z}{1+Z} = \varepsilon \quad (18)$$

where C_ε' is a model constant of about 1.2 and ν_{fl} the kinematic viscosity for a gaseous phase. The first term represents the viscous dissipation by the presence of particles and the second term approximates the rate of energy dissipation due to the fluctuating relative velocities per unit mass of the bulk fluids, and the right-hand side of equation (18) is the rate of dissipation for suspension flow.

Near the viscous sublayer, the turbulent Reynolds number is very small, and thus, the peak of the dissipation spectrum and the peak of the spectrum of the energy containing eddies approach the same order (see Fig. 7.6 in ref. [16]). Lumley [16] proposed that the viscous cutoff wave number under particle loading is proportional to $[(s/\nu_{fl})(1+Z)]^{1/2}$ and the ratio of the viscous cutoff wave number k_d of the suspension to that in the clean gas flow is given by $\hat{k}_d = [\hat{s}(1+Z)]^{1/2}$, where $\hat{s} = s(\nu_{fl}/\varepsilon)^{1/2}$. Further, it is proposed that since the ratio of sublayer thickness under particle loading to that in the clean gas flow $\hat{\delta}$ is $\hat{k}_d^{-4/3}$, the drag reduction viscous sublayer thickness A_{DR}^+ can be expressed as follows:

$$A_{DR}^+ = \delta_o^+\hat{\delta} = \delta_o^+\hat{k}_d^{-4/3} \quad (19)$$

where δ_o^+ is the viscous sublayer thickness in clean gas flow.

Since it is assumed that the turbulence is suppressed by the presence of particles, A^+ must be greater than or equal to that of the clean gas flow. Thus, the present authors [14] proposed that the damping constant may be determined as follows:

$$A^+ = A_o^+ \quad \text{for } A_o^+ > A_{DR}^+ \quad (20)$$

$$A^+ = A_{DR}^+ \quad \text{otherwise} \quad (21)$$

where A_o^+ is an effective viscous sublayer in clean gas flows. It is found that the above model equations (20) and (21) yields the best agreement with the experimental data [17] in the previous study [14].

The eddy viscosity of the particulate phase ε_p and the virtual laminar kinematic viscosity of the particulate phase ν_{pl} are modelled by the proposal given in ref. [23].

Thermal eddy diffusivity models

The thermal eddy diffusivity of the gaseous phase λ_f due to the suspension of particles can be derived using the similar method for deriving the scalar eddy viscosity ε_f [15]. From the governing equation of the mean temperature variance $\overline{\theta_f^2}$ for the gaseous phase, the production term P_θ and its dissipation term ε_θ can be approximated as follows:

$$P_\theta = \overline{\rho_f}\lambda_f\left(\frac{dT_f}{dr}\right)^2 \quad (22)$$

$$\varepsilon_\theta = \rho_f\alpha_{fl}\overline{\frac{\partial\theta_f}{\partial r}\frac{\partial\theta_f}{\partial r}} + K_\theta\frac{\rho_p}{\tau^*}\frac{C_{p_p}}{C_{p_f}}\overline{\theta_f(\theta_f-\theta_p)} \quad (23)$$

where α_{fl} is the laminar thermal diffusivity for the gaseous phase and the bulk density of the particulate matter is assumed to be constant.

Using appropriate relations

$$\theta_f \approx l_{fh}\,dT_f/dr$$

$$\alpha_{fl}\overline{\frac{\partial\theta_f}{\partial r}\frac{\partial\theta_f}{\partial r}} \approx u_f\frac{\overline{\theta_f^2}}{l_{fh}}$$

and

$$Pr_{T_{fo}} \approx l_f/l_{fh}$$

the assumption of the local state of equilibrium of the mean temperature variance for the gaseous phase ($P_\theta = \varepsilon_\theta$) yields the thermal eddy diffusivity as follows:

$$\frac{\varepsilon_f}{\lambda_f} = Pr_{T_f} = \left[\frac{Pr_{T_{fo}}}{1+\dfrac{a}{Pr_{T_{fo}}}\dfrac{t_l}{\tau^*}\dfrac{\overline{\rho_p}}{\overline{\rho_f}}\dfrac{C_{p_p}}{C_{p_f}}\left(1-\dfrac{\overline{\theta_p^2}}{\overline{\theta_f^2}}\right)}\right] \quad (24)$$

where a is a model constant of about 1.0, l_{fh} the thermal characteristic length scale for the gaseous phase, and $Pr_{T_{fo}}$ the turbulent Prandtl number of the clean gas without particles.

The ratio of the temperature variances $\overline{\theta_p^2}/\overline{\theta_f^2}$ in the above equation (24) is modelled by Tien [24] as

$$\frac{\overline{\theta_p^2}}{\overline{\theta_f^2}} = \frac{1}{1+\dfrac{1}{\sqrt{3}}\left(\dfrac{\tau^*}{t_l}\right)}. \quad (25)$$

The modelling of $Pr_{T_{fo}}$ is done by a correlation formulae proposed by Crawford and Kays [25]

$$Pr_{T_{fo}} = \left[\frac{B^2}{2} + 0.2B\,Pe - (0.2Pe)^2\left\{1-\exp\left(\frac{B}{0.2Pe}\right)\right\}\right]^{-1}. \quad (26)$$

Here, Pe is the turbulent Peclet number and B an empirical constant of about 1.08.

The turbulent Prandtl number for the particulate phase Pr_{T_p} is taken to be 0.9 according to Abou-Arab and Abou-Ellail [13].

Finally, the concept of virtual laminar thermal diffusivity of the particulate phase needs some deliberation. It can be safely assumed that, since the particles and the wall are pointly contacted, direct heat transfer from the hot wall to the solid particle near the wall is practically negligible. Therefore, it may be assumed that the particulate phase does not have any virtual laminar thermal diffusivity. A consequence of this view of the heat transfer mechanism is that the temperature rise of the solids lags behind that of the gas; i.e. the gas temperature rises first and then the particle temperature rises due to the heat transfer between particles and the surrounding heated gas.

BOUNDARY AND INITIAL CONDITIONS

Due to the no-slip condition at the wall, the wall boundary conditions of the gaseous phase are given by

$$U_f = V_f = 0; \quad T_f = T_w. \quad (27)$$

On the other hand, the particles may be in slip motion at the wall. Assuming that the particle mass is concentrated pointly at the centre of the particle, particles cannot exist in the region within the distance from the wall smaller than the radius of the particle. Therefore, the velocities and temperature for the particulate phase at the wall may be approximated as follows:

$$U_p = U_{f,\,r=d_p/2}; \quad V_p = 0$$

$$T_p = T_{f,\,r=d_p/2}. \quad (28)$$

For the wall boundary condition of the concentration for the particulate phase, a Neumann condition, $d\overline{\rho_p}/dr = 0$, is specified for mathematical simplicity.

On the axis of symmetry, the symmetry conditions are imposed on U_f, U_p, T_f, T_p and $\overline{\rho_p}$. In addition, the radial velocities V_f and V_p are set to zero.

The velocity profiles for both phases and the particulate density profile in the fully developed region without heat transfer, which were calculated by the present authors [14], were used as the inlet conditions into the heating section. The suspension local Nusselt number is defined as

$$Nu_s = \frac{h_s D}{k_f} = \frac{\dot{q}'' D}{(T_w - T_{mm})k_f}. \quad (29)$$

Here, the mixed mean temperature of the suspension $T_{mm}(x)$ is calculated using

$$T_{mm}(x) = \frac{\int C_{p_f}\overline{\rho_f}U_f T_f\,dA + \int C_{p_p}\overline{\rho_p}U_p T_p\,dA}{\int C_{p_f}\overline{\rho_f}U_f\,dA + \int C_{p_p}\overline{\rho_p}U_p\,dA}. \quad (30)$$

The thermal conductivity of the gaseous phase k_f is evaluated at the film temperature $(T_w + T_{mm})/2$ [6, 7].

COMPUTATIONAL RESULTS AND DISCUSSION

In order to verify the accuracy of our thermal eddy diffusivity model, together with Lumley's drag reduction theory, computations are carried out for the experiments of Boothroyd and Haque [6, 7] with an average particle size of 15 μm at a gas Reynolds number of 53 000.

Figure 1 compares predicted suspension Nusselt numbers with the experimental data [7] in the fully developed region ($x = 3.048$ m) with constant wall heat flux ($\dot{q}'' = 2888.3\ \mathrm{W\,m^{-2}}$). As the relative particle size d_p/D increases, the suspension Nusselt number in the case $d_p/D = 5.91 \times 10^{-4}$ is markedly reduced below the value for clean gas flow. At the same relative particle size, the suspension Nusselt number first reduces and then increases with an increase in the loading ratio. These phenomena are similar to those of the skin friction factor in Fig. 2 of ref. [14].

Figure 2 shows evaluations of the effective non-dimensional sublayer thickness for the suspension flow with and without heat transfer using equations (20) and (21). It can be seen that A^+ with heat transfer is less than A^+ without heat transfer. This is due to the variation of near wall gas properties such as the absolute viscosity and the density. Increase of the absolute viscosity and decrease of the gas density near the wall region reduce particle relaxation time and augment the local density ratio $(\overline{\rho_p}/\overline{\rho_f})$, respectively. An increase of A^+ means stronger resistance to the

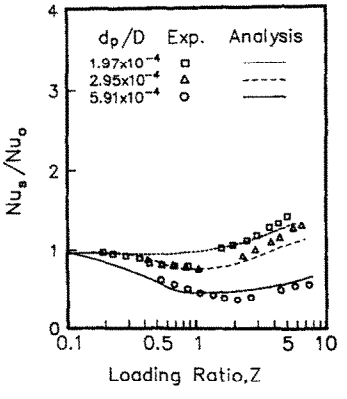

FIG. 1. Comparison of predicted suspension Nusselt numbers with those of experiments by Boothroyd and Haque [7].

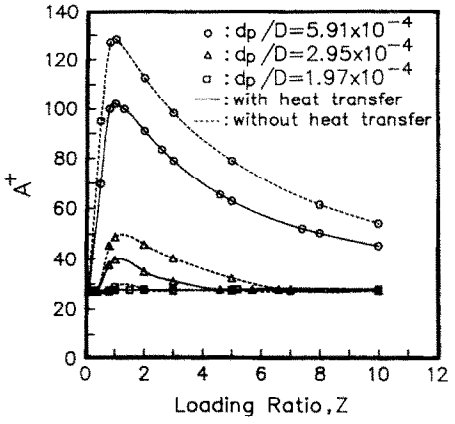

FIG. 2. Estimations of the effective non-dimensional sublayer thicknesses with and without heat transfer using equations (20) and (21).

heat transfer and thus the suspension Nusselt number decreases under the particle loading; particularly, its effect is predominant for the loading ratio near unity.

Computed mean temperature profiles of the gaseous phase for various relative particle sizes at $x = 3.048$ m downstream from the thermal entrance are shown in Figs. 3(a)–(c) with the solids–gas loading ratio as a parameter. When the loading ratio increases, the temperature in the core region becomes lower than that of clean gas ($Z = 0$). However, the temperature near the wall region significantly varies according to the relative particle size and loading ratio. Because the temperature difference between the gaseous and particulate phases in Boothroyd and Haque's experiments [6, 7] is small, the temperature profiles of the particulate phase are not represented in this paper.

Figure 4 displays the spatial distributions of particulate phase density normalized by that at the centreline for $d_p/D = 1.97 \times 10^{-4}$ and 5.91×10^{-4}. From this figure, it can be seen that the particles distribute nearly uniformly for small relative particle size. However, for high relative particle size, particles are more concentrated in the core region. Note the sharp variation of the particulate phase density near the wall region as shown in details in the inset of Fig. 4, which is qualitatively consistent with the Lagrangian simulation of Kallio and Reeks [26] (see Fig. 5 in ref. [26]).

Figures 5(a) and (b) represent the mean axial velocity profiles of the gaseous phase normalized by the centreline mean velocity of the clean gas in $d_p/D = 1.97 \times 10^{-4}$ and 5.91×10^{-4}. As loading ratio increases, the centreline velocity increases, while the velocity near the wall layer decreases. Because part of the heat is transferred to the particulate phase, the bulk temperature of the gaseous phase is lower than that of clean gas flow. Therefore, the density at the bulk temperature is higher than that of clean gas flow. Thus, the mean axial velocity of the gaseous phase with particle loading is always slower than that of the clean gas flow from the mass continuity of the gaseous phase.

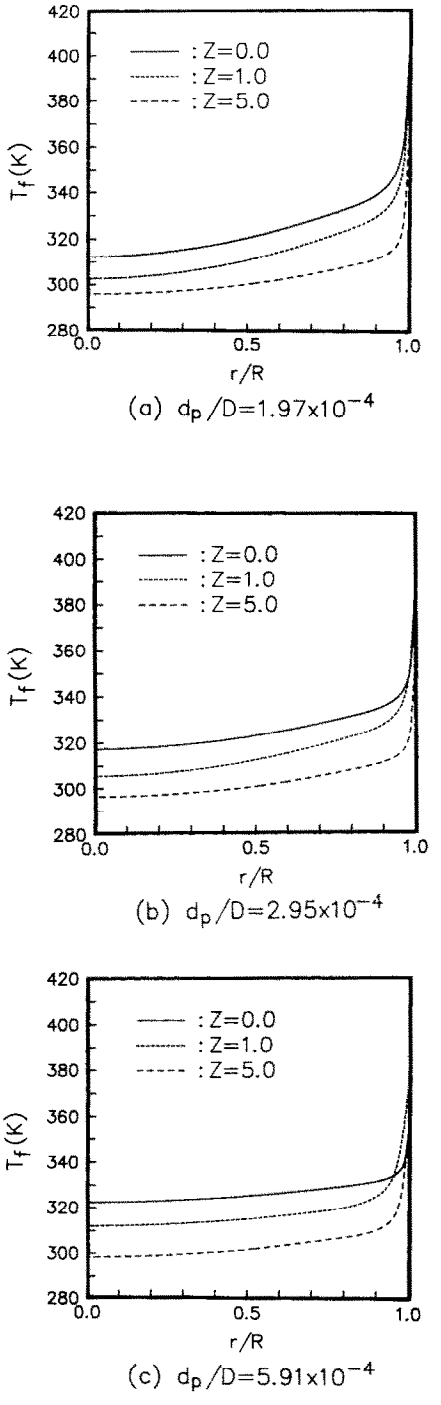

FIG. 3. Mean temperature profiles of the gaseous phase for various relative particle sizes and loading ratios at $x = 3.048$ m from the thermal entry: (a) $d_p/D = 1.97 \times 10^{-4}$; (b) $d_p/D = 2.95 \times 10^{-4}$; (c) $d_p/D = 5.91 \times 10^{-4}$.

Dependency of the centreline turbulent Prandtl number $(Pr_T)_c$ on the loading ratio and the relative particle size are calculated from equation (24) and the results are shown in Fig. 6, which reveals that the

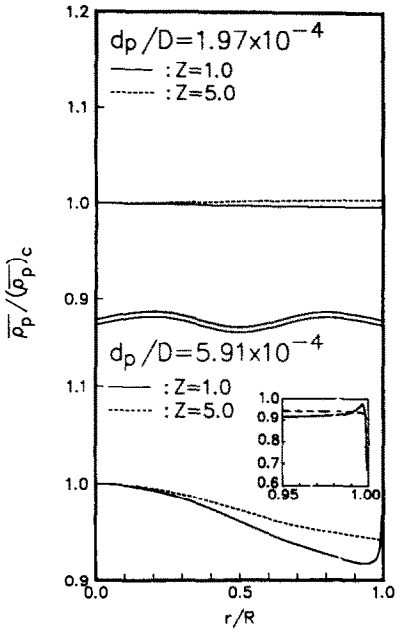

FIG. 4. Normalized spatial distributions of particulate phase density for various relative particle sizes and loading ratios.

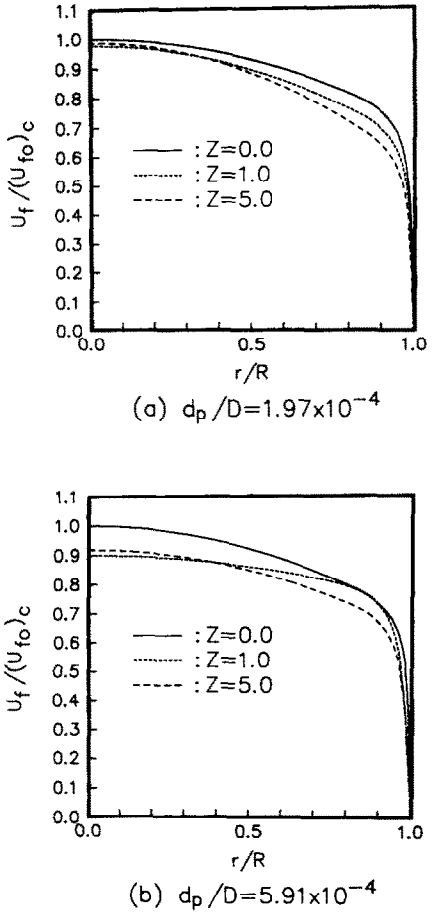

FIG. 5. Normalized mean axial velocity profiles of the gaseous phase for various relative particle sizes and loading ratios: (a) $d_p/D = 1.97 \times 10^{-4}$; (b) $d_p/D = 5.91 \times 10^{-4}$.

turbulent Prandtl number decreases monotonically with increasing Z and decreasing d_p/D. Such an appreciable decrease in Pr_{T_f} implies that loading of particles in the gas stream makes the transfer of energy by the bulk fluid much faster than that of momentum. Note that the suspension turbulent Prandtl number in the present study includes a heat capacity–density ratio $\rho_p C_{p_p}/\rho_f C_{p_f}$ as in the experimental correlation of Michaelides and Lasek [11] (see equation (11) in ref. [11]).

Figure 7 depicts the radial distributions of the turbulent Prandtl number. It can be seen that the turbulent Prandtl number in the suspension is much smaller than that of the clean gas in the whole region, and that it is nearly constant in the core region, while it rapidly increases approaching the wall. For large relative particle size, the location at which Pr_{T_f} rapidly increases moves to the pipe core due to the increase of the sublayer thickness as in Fig. 2.

Figures 8(a) and (b) show comparisons between the experimental [6] and computational results for axial variations of the suspension Nusselt numbers under various loading ratios. The solid lines are the present computational results and the symbols indicate experimental data, both of which are in satisfactory agreement with each other.

Finally, the computed axial variations of the wall temperature and the bulk temperature of the gaseous phase are drawn in Figs. 9(a) and (b). When the solids–gas loading ratio is increased, it can be seen that the bulk temperature of the gaseous phase increases slower than that of the clean gas, while the comparison of the wall temperature variation under particle loading with that of clean gas does not show any consistent

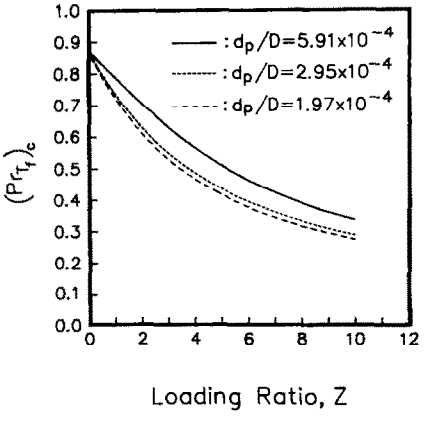

FIG. 6. Predicted turbulent Prandtl number in the core region for the gaseous phase as a function of loading ratio and the relative particle size.

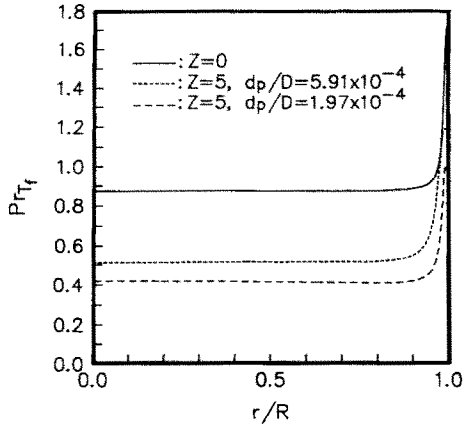

FIG. 7. Predicted turbulent Prandtl number distributions for the gaseous phase for different relative particle size.

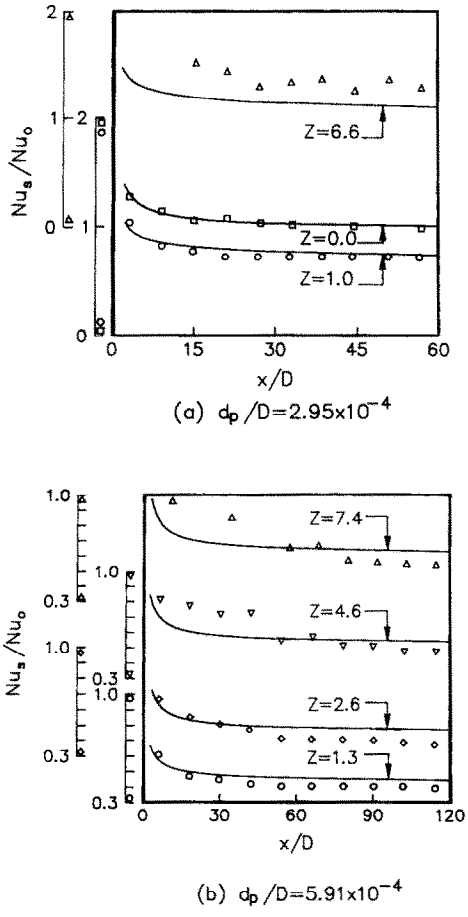

FIG. 8. Comparisons of predicted axial variations of the suspension Nusselt numbers at $Re = 5.3 \times 10^4$ with the experiments of Boothroyd and Haque [6]: (a) $d_p/D = 2.95 \times 10^{-4}$; (b) $d_p/D = 5.91 \times 10^{-4}$. (Sliding ordinate scales used.)

trend. The latter comparison is rather complicated and must be explained with the aid of the information about the sublayer thickness and the heat capacity–density ratio $\overline{\rho}_p C_{p_p}/\overline{\rho}_f C_{p_f}$, which are two important factors for suspension heat transfer. Increase of the sublayer thickness leads to the reduction of the suspension heat transfer, while that of the heat capacity–density ratio augments the heat transfer. From Fig. 2, for the loading ratio near unity, the sublayer thickness significantly varies according to the relative particle size, while the effect of heat capacity–density ratio is relatively small. Therefore, if sublayer thickness increases, the wall temperature of the gaseous phase becomes higher than that of clean gas. For higher particle loading, the effect of $\overline{\rho}_p C_{p_p}/\overline{\rho}_f C_{p_f}$ becomes more important, while the variation of the sublayer thickness is relatively small. Therefore, if the latter is the case, variation of the wall temperature of the gaseous phase becomes more dependent on the heat capacity–density ratio, and consequently, the wall temperature of the suspension becomes lower than that of clean gas flow.

CONCLUSIONS

In order to investigate numerically the heat transfer of gas–particle two-phase flows in a vertical pipe, Lumley's drag reduction theory and a new thermal eddy diffusivity model are employed in a previous two-fluid model. The thermal eddy diffusivity model for the gaseous phase was derived from an approximate balance equation for the mean temperature variance $\overline{\theta_f^2}$ of the gaseous phase. It turns out that there are two important factors for the suspension heat transfer; one is the sublayer thickness and the other is the heat capacity–density ratio $\rho_p C_{p_p}/\rho_f C_{p_f}$. Application of the proposed two-fluid model to several suspension heat transfer problems under various conditions yield satisfactory predictions for the dependency of Nusselt number on the relative particle size, particle loading ratio and on the axial distance from the thermal entry.

As relative particle size increases, the suspension Nusselt number is significantly reduced. The addition of solid particles to the flowing gas in a pipe affects the size of the sublayer thickness and the heat capacity–density ratio. The major cause of decrease in the suspension Nusselt number at low particle loading is mainly due to the increase of the viscous sublayer thickness caused by the suppression of turbulence near the wall. But, in high loading, the effect of the heat capacity–density ratio becomes more important and augments the suspension heat transfer. The effective non-dimensional sublayer thickness with heat transfer is thinner than that without heat transfer. As loading ratio increases, the temperature in the core region becomes lower than that of the clean gas. The suspension turbulent Prandtl number of the gaseous phase is affected by the heat capacity–density ratio and the ratio of times scales τ^*/t_l. As the ratio $\rho_p C_{p_p}/\rho_f C_{p_f}$ increases, the suspension turbulent Prandtl number of the gaseous phase considerably decreases.

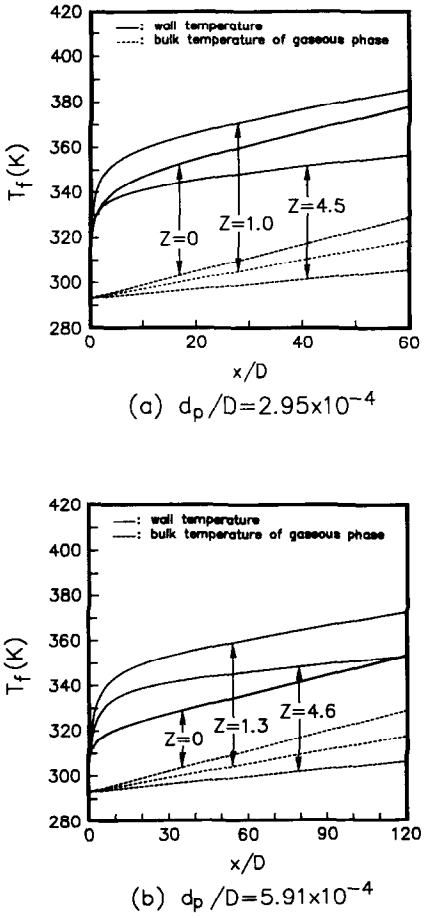

FIG. 9. Computed axial variations of the wall and the bulk temperatures of the gaseous phase: (a) $d_p/D = 2.95 \times 10^{-4}$; (b) $d_p/D = 5.91 \times 10^{-4}$.

All these findings from the computed results could be confirmed by comparing them with available experimental data.

REFERENCES

1. L. Farbar and M. J. Morley, Heat transfer to flowing gas–solids mixtures in a circular tube, *Ind. Engng Chem.* **49,** 1143–1150 (1957).
2. G. T. Wilkinson and J. R. Norman, Heat transfer to a suspension of solids in a gas, *Trans. Instn Chem. Engrs* **45,** 314–318 (1967).
3. L. Farbar and C. A. Depew, Heat transfer effects to gas–solids mixtures using solid spherical particles of uniform size, *I&EC Fundam.* **2,** 130–135 (1963).
4. C. A. Depew and L. Farbar, Heat transfer to pneumatically conveyed glass particles of fixed size, *Trans. ASME*, Series C, *J. Heat Transfer* **85,** 164 172 (1963).
5. M. K. Wahi, Heat transfer to flowing gas–solids mixtures, *Trans. ASME*, Series C, *J. Heat Transfer* **99,** 145–148 (1977).
6. R. G. Boothroyd and H. Haque, An experimental investigation of heat transfer in the entrance region of a heated duct conveying fine particles, *Trans. Instn Chem. Engrs* **48,** 109–120 (1970).
7. R. G. Boothroyd and H. Haque, Fully developed heat transfer to a gaseous suspension of particles flowing turbulently in ducts of different size, *J. Mech. Engng Sci.* **12,** 191–200 (1970).
8. R. S. Kane and R. Pfeffer, Heat transfer in gas–solids drag-reducing flow, *Trans. ASME*, Series C, *J. Heat Transfer* **107,** 570–574 (1985).
9. C. L. Tien, Heat transfer by a turbulently flowing fluid–solids mixture in a pipe, *Trans. ASME*, Series C, *J. Heat Transfer* **83,** 183–188 (1961).
10. E. E. Michaelides, Heat transfer in particulate flows, *Int. J. Heat Mass Transfer* **29,** 265–273 (1986).
11. E. E. Michaelides and A. Lasek, Fluid–solids flow with thermal and hydrodynamic non-equilibrium, *Int. J. Heat Mass Transfer* **30,** 2663–2669 (1987).
12. T. W. Abou-Arab, Turbulence models for two-phase flows. In *Encyclopedia of Fluid Mechanics* (Edited by N. P. Cheremisinoff), Vol. III, pp. 863–904. Gulf, New Jersey (1985).
13. T. W. Abou-Arab and M. M. M. Abou-Ellail, Computation of heat and momentum transfer in turbulent gas/solid flows, *Proc. Int. Symp. of Multiphase Flows*, Hangzhou, China, pp. 374–379 (1987).
14. K. S. Han, M. K. Chung and H. J. Sung, Application of Lumley's drag reduction model to two-phase gas–particle flow in a pipe, *Trans ASME, J. Fluids Engng* (in press).
15. K. B. Lee and M. K. Chung, Refinement of the mixing-length model for prediction of gas–particle flow in a pipe, *Int. J. Multiphase Flow* **13,** 275–282 (1987).
16. J. L. Lumley, Two-phase and non-Newtonian flows. In *Topics in Applied Physics*, Vol. 12, *Turbulence* (Edited by P. Bradshaw), Chap. 7. Springer, Berlin (1976).
17. R. G. Boothroyd, Pressure drop in duct flow of gaseous suspensions of fine particles, *Trans. Instn Chem. Engrs* **44,** 306–313 (1966).
18. M. Ishii, *Thermo-fluid Dynamic Theory of Two-phase Flow*. Eyrolles, Paris (1975).
19. F. E. Marble, Dynamics of dusty gases, *Ann. Rev. Fluid Mech.* **2,** 397–446 (1970).
20. M. A. Rizk and S. E. Elghobashi, The motion of a spherical particle suspended in a turbulent flow near a plane wall, *Physics Fluids* **28,** 806–817 (1985).
21. M. P. Sharma and C. T. Crowe, A novel physico-computational model for quasi one-dimensional gas–particle flows, *Trans. ASME*, Series I, *J. Fluids Engng* **100,** 343–349 (1978).
22. R. G. Boothroyd, *Flowing Gas–Solids Suspensions*. Chapman & Hall, London (1971).
23. Y. D. Choi and M. K. Chung, Analysis of turbulent gas–solid suspension flow in a pipe, *Trans. ASME*, Series I, *J. Fluids Engng* **105,** 329–334 (1983).
24. C. L. Tien, Transport processes in two-phase turbulent flow, Ph.D. thesis, Princeton University, Princeton, New Jersey (1959), cited from S. L. Soo, *Fluid Dynamics of Multiphase Systems*, pp. 60–69. Blaisdell (1967).
25. M. E. Crawford and W. M. Kays, A program for numerical computation of two dimensional internal/external boundary layer flows, Rept. HMT-23, Stanford University, California (1975).
26. G. A. Kallio and M. W. Reeks, A numerical simulation of particle deposition in turbulent boundary layers, *Int. J. Multiphase Flow* **15,** 433–446 (1989).

ANALYSE DE TRANSFERT THERMIQUE DANS UN TUYAU TRANSPORTANT UNE SUSPENSION DIPHASIQUE GAZ PARTICULES

Résumé—Un modèle à deux fluides utilisant le concept de diffusivité turbulente et la théorie de réduction de trainée selon Lumley est proposé pour analyser le transfert thermique de l'écoulement turbulent gaz particules diluées dans un tuyau vertical avec flux thermique pariétal uniforme. Le modèle de diffusivité thermique turbulente est une fonction du rapport des produits $\bar{\rho}C_p$ (capacité thermique masse volumique) de la phase gazeuse et de la phase de particules et aussi du rapport du temps de relaxation thermique à celui de la turbulence. La théorie de Lumley est appliquée pour trouver la variation de l'épaisseur de la sous-couche visqueuse qui dépend du rapport de charge de particules Z et de la taille relative de particules d_p/D. Aux faibles rapports de charge, la taille de l'épaisseur de la sous-couche visquese est importante pour le transfert thermique de la suspension, tandis qu'aux plus fortes charges, l'effet du rapport $\bar{\rho}_p C_{p_p}/\bar{\rho}_f C_{p_f}$ est dominant. La cause principale de la décroissance du nombre de Nusselt de la suspension aux faibles rapports de charge est due à l'augmentation de l'épaisseur de la sous-couche visqueuse, elle-même due à la suppression de la turbulence près de la paroi par la présence des particules solides. Les nombres de Nusselt calculés à partir de ce modèle sont en accord satisfaisant avec les données expérimentales à la fois à l'entrée du tube et dans les régions pleinement établies.

BERECHNUNG DES WÄRMEÜBERGANGS IN EINEM ROHR MIT EINER ZWEIPHASIGEN GAS/PARTIKEL-SUSPENSION

Zusammenfassung—Es wird ein Zwei-Fluid-Modell für die Berechnung des Wärmeübergangs in einer turbulenten Strömung aus verdünntem Gas und Partikeln in einem senkrechten Rohr bei konstanter Wärmestromdichte an der Wand vorgeschlagen. Dabei finden das Konzept der wirbelbedingten Scheintemperaturleitfähigkeit und die Theorie der Widerstandsverminderung nach Lumley Verwendung. Es wird gezeigt, daß das Modell der Scheintemperaturleitfähigkeit vom Verhältnis der volumetrischen Wärmekapazitäten der Gasphase und der Partikel abhängt, außerdem vom Verhältnis der thermischen Relaxationszeit-Skala zu derjenigen der Turbulenz. Lumley's Theorie wird dazu verwendet, die Abhängigkeit der Dicke der viskosen Unterschicht vom Beladungsverhältnis Z mit Partikeln und von der relativen Partikelgröße d_p/D zu ermitteln. Bei kleinen Beladungsverhältnissen ist die Dicke der viskosen Unterschicht wichtig für den Wärmeübergang in der Suspension, während bei großen Beladungsverhältnissen der Einfluß des Verhältnisses der volumetrischen Wärmekapazitäten dominiert. Der Hauptgrund für das Abnehmen der Nusselt-Zahl der Suspension bei geringen Beladungsverhältnissen ist auf ein Anwachsen der Dicke der viskosen Unterschicht zurückzuführen, was auf einer Unterdrückung der Turbulenz nahe an der Wand infolge der Anwesenheit von Feststoffpartikeln zurückzuführen ist. Die mit dem vorgestellten Modell berechneten Nusselt-Zahlen stimmen befriedigend mit verfügbaren Versuchsdaten überein; dies gilt sowohl im Einlaufgebiet wie auch im Bereich der vollständig entwickelten Strömung.

АНАЛИЗ ТЕПЛОПЕРЕНОСА В ТРУБЕ С ДВУХФАЗНОЙ СМЕСЬЮ ГАЗА И ЧАСТИЦ

Аннотация—Предложена "модель двух жидкостей", использующая понятие турбулентной температуропроводности и теорию уменьшения сопротивления Ламбли, для анализа теплопереноса турбулентного потока газа и частиц в вертикальной трубе с постоянным тепловым потоком на стенке. Найдено, что турбулентная температуропроводность является функцией отношения произведений теплоемкостей и плотностей частиц и газообразной фазы $\bar{\rho}C_p$, а также отношения временных масштабов тепловой релаксации и турбулентности. Теория Ламбли применяется для определения изменения толщины вязкого подслоя в зависимости от концентрации частиц Z и их относительного размера d_p/D. При низкой концентрации толщина вязкого подслоя является существенной для теплопереноса в суспензиях, в то время как при более высоких концентрациях доминирующее влияние оказывает отношение $\bar{\rho}_p C_{p_p}/\bar{\rho}_f C_{p_f}$. Найдено, что основной причиной уменьшения числа Нуссельта в случае низкой концентрации является рост толщины вязкого подслоя за счет подавления турбулентности вблизи стенки твердыми частицами. Значения числа Нуссельта, рассчитанные по предложенной модели, удовлетворительно согласуются с имеющимися экспериментальными данными для входного участка трубы и полностью развитых областей.